The Canadian Mineralogist
Vol. 42, pp. 1847-1857 (2004)

RECRYSTALLIZATION OF METAMICT Nb–Ta–Ti–REE COMPLEX OXIDES: A COUPLED X-RAY-DIFFRACTION AND RAMAN SPECTROSCOPY STUDY OF AESCHYNITE-(Y) AND POLYCRASE-(Y)

NENAD TOMAŠIĆ[§]

Institute of Mineralogy and Petrography, Faculty of Science, University of Zagreb, Horvatovac bb, HR-10000 Zagreb, Croatia

ANDREJA GAJOVIĆ

Rudjer Bošković, Institute, Division of Materials Physics, Molecular Physics Laboratory, Bijenička cesta 54, HR-10002 Zagreb, Croatia

VLADIMIR BERMANEC

Institute of Mineralogy and Petrography, Faculty of Science, University of Zagreb, Horvatovac bb, HR-10000 Zagreb, Croatia

MAŠA RAJIĆ

Brodarski Institut, HR-10000 Zagreb, Croatia

ABSTRACT

Metamict aeschynite-(Y) and polycrase-(Y) were studied by X-ray diffraction and Raman spectroscopy. To restore their crystal structure, the mineral samples were heated at various temperatures in air. The temperatures of 400, 500, 650, 800 and 1000°C were determined from TGA–DTA diagrams to be potentially important for structure restoration or changes, which generally correspond to the data available from previous studies. Raman spectroscopy was used to discover possible vibration bands characteristic of the metamict minerals investigated. The changes of vibration spectra are due to heating, but also reveal possible features of the crystal structure not observable by X-rays. Both X-ray diffraction and Raman spectroscopy data indicate a gradual increase in crystallinity with temperature increase. Transformation from the aeschynite to euxenite structure was observed for both minerals, but up to 1000°C, it is incomplete for aeschynite-(Y) and complete for polycrase-(Y). Raman spectra of both minerals are generally similar, a reflection of their similar chemical and structural properties, but the differences observed probably arise because of the different way the coordination polyhedra are stacked. These differences are the most pronounced in the wavenumber region from 200 to 550 cm^{-1}, which is suitable for fingerprint recognition of the mineral phases with the aeschynite or euxenite structure.

Keywords: aeschynite-(Y), polycrase-(Y), metamictization, recrystallization, crystal-structure transformation, X-ray-diffraction, Raman spectroscopy, thermogravimetry.

SOMMAIRE

Nous avons étudié l'aeschynite-(Y) et le polycrase-(Y) métamictes par diffraction X et par spectroscopie de Raman. Afin de rétablir leur structure originelle, ces échantillons ont été chauffés à divers paliers de température. Les températures 400, 500, 650, 800 et 1000°C semblent, d'après les tracés thermogravimétriques et thermiques différentiels, être des étapes importantes dans la restauration ou le changement des structures, qui correspondent en général aux données déjà disponibles. Nous nous sommes servis de la spectroscopie de Raman pour découvrir des bandes de vibration possiblement caractéristiques des minéraux métamictes étudiés. Les changements de vibration dans ces spectres sont dus au réchauffement, mais révèlent aussi des effets possibles sur la structure non observables par rayons X. Les données en diffraction X et les spectres de Raman indiquent une augmentation graduelle de la cristallinité à mesure qu'augmente la température. Nous observons une transformation de la structure de l'aeschynite à celle de l'euxénite dans les deux minéraux, mais en chauffant jusqu'à 1000°C, elle est incomplète pour

§ *E-mail address*: ntomasic@jagor.srce.hr

l'aeschynite-(Y) et complète pour le polycrase-(Y). Les spectres de Raman des deux minéraux sont semblables, réflexion de leur ressemblance chimique aussi bien que structurale, mais les différences observées dépendraient surtout de la façon dont les polyèedres de coordinence sont empilés. Ces différences sont le plus prononcées dans l'intervalle de fréquence entre 200 et 550 cm^{-1}, qui semble approprié pour reconnaître les phases minérales ayant la structure de l'aeschynite ou de l'euxénite.

(Traduit par la Rédaction)

Mots-clés: aeschynite-(Y), polycrase-(Y), métamictisation, recristallisation, transformation cristalline, diffraction X, spectroscopie de Raman, thermogravimétrie.

Introduction

Complex Nb–Ta–Ti–REE oxide minerals are of great interest owing to their significance as monitors of petrological evolution and geochemical processes in their host rocks, generally granitic pegmatites. These minerals are also of interest with respect to their usual metamict state. In this work, we focus on metamict aeschynite-(Y) and polycrase-(Y). The general chemical formula for both aeschynite and polycrase is AB_2O_6, where *A* represents the rare-earth elements (REE), Ca, Th and U, and *B* stands for Ti, Nb and Ta. Both minerals are orthorhombic, but aeschynite-(Y) crystallizes in space group *Pbnm*, which is characteristic of the minerals of the aeschynite group, whereas polycrase-(Y) has the euxenite structure, with the space group *Pbcn*; it thus belongs to the euxenite group, and considered the Ti-dominant analogue of euxenite.

Our aim in this work is to study the recrystallization of the metamict Nb–Ta–Ti–REE complex oxides using X-ray diffraction and Raman spectroscopy. Such a combined approach is intended (1) to monitor more thoroughly the recrystallization process occurring with increase in temperature, (2) to reveal more information about the degree of disorder of the minerals in the metamict state, and (3) to get information on the possible crystal-structure features invisible to traditionally employed X-ray-diffraction investigations of metamict minerals.

Background Information

As described by Berman (1955), the term "metamict" refers to the "noncrystalline pseudomorphs of material presumed to have been crystalline originally". Mainly, radiation damage of the structure is the reason for metamict state (Ewing 1975, 1987). Unstable nuclei of U or Th (or both) present in a mineral produce α-particles, which dissipate their energy by ionization and limited elastic collisions along their path. As a result, isolated defects with several hundred atomic displacements are formed. The remaining nuclei recoil in opposite direction, causing collisional cascades with a few thousand atomic displacements (Ewing 1987, Gögen & Wagner 2000). Alpha recoil nuclei cause most of the displacements responsible for amorphization of crystal structures (Ewing *et al.* 1995, Nasdala *et al*. 2002, Seydoux-Guillaume *et al.* 2002). However, it is still unclear why some minerals, for example monazite, containing significant amounts of U and Th, never appear naturally in the metamict state. Graham & Thornber (1974) proposed another factor to consider: complex niobium and tantalum oxides have a complex chemical composition, which could cause imbalances in the crystal structure and segregation of simple phases into microregions.

Early investigators of metamict minerals found that it is possible to recrystallize them by heating. The optimal conditions, temperatures of recrystallization, and X-ray- diffraction patterns of heated metamict minerals have been investigated in the works of Arnott (1950), Berman (1955), Lima de Faria (1958, 1962), among others. Investigations using Raman spectroscopy investigations, as a powerful tool to study the state of order in minerals, in particular in metamict minerals, do not have such a long history. So far, metamict zircon and monazite have been investigated mainly. Nasdala *et al.* (1995, 2002) investigated a series of crystalline and metamict samples of zircon and showed how the half-widths of Raman bands could be used to estimate the degree of metamictization. Seydoux-Guillaume (2001) used Raman spectroscopy to study disordered but not metamict monazite-group minerals, which are not commonly found to be metamict (Ewing 1975). As in the case of zircon, the degree of order in the crystal structure was assessed through the width of Raman bands (Seydoux-Guillaume 2001, Seydoux-Guillaume *et al*. 2002). Actinide-bearing monazite was investigated by Podor (1995), who found that the increase in the U:Th ratio of monazite increases the wavenumber of the symmetric stretch bands of the PO_4^{3-} group.

Raman spectroscopy has not been widely employed in the investigation of the metamict complex oxides. Therefore, the reference data for their vibration spectra are not available, and interpretations and band assignments must be treated with caution. Theoretical estimations and calculations of vibration spectra for the complex oxides are very complicated, especially if the number of possible substitutions into cation sites in the crystal structure is considered. However, it is possible to predict the number of Raman-active modes (number of bands in the spectra) using group-theory analysis. On the other hand, it is promising to look for similarities between Raman spectra of synthetic compounds with a

corresponding crystal-structure or similar chemical composition.

Recently, Paschoal *et al.* (2003) conducted a study of Raman scattering on $REETiTaO_6$ ceramics with aeschynite- and euxenite-type structures. Raman studies of lanthanide oxides (White & Keramidas 1972, Boldish & White 1979, Tucker *et al.* 1984) and niobium oxides (McConnell *et al.* 1976) also give interesting Raman data pertaining to complex synthetic systems, for instance on layered titanium oxides including sodium and lanthanides (Byeon *et al.* 1997), on the system Ta_2O_5–TiO_2 (Meng *et al.* 1997) and on the system Y_2O_3–Nb_2O_5 (Yashima *et al.* 1997).

Description of the Samples

Samples of both minerals investigated originate from granitic pegmatites situated in the Aust–Agder province of southern Norway. Aeschynite-(Y) was collected in the Tuftane granitic pegmatite, situated in the Iveland district. Polycrase-(Y) was found in the Kjælevann granitic pegmatite, Birkenes district. The granitic pegmatites of this region were intruded in the Precambrian amphibolites and gneisses (Bugge 1978). The pegmatites are famous for a variety of rare minerals [davidite-(Ce), gadolinite-(Y), allanite-(Ce), euxenite-(Y), aeschynite-(Y), polycrase-(Y), thortveitite] associated with microcline, plagioclase, quartz, biotite and muscovite (Neumann & Sverdrup 1960).

Both aeschynite-(Y) and polycrase-(Y) occur as masses up to a few centimeters across, without crystal faces. They are black with a vitreous luster and a conchoidal fracture. Where broken to thin splinters, they are reddish and translucent. The metamict samples were chosen for the investigation in view of (1) their very similar chemical composition, characterized by the predominance of Y and Ti, (2) their related but different structures, and (3) the aeschynite–euxenite phase transition that occurs as the minerals are heated.

Experimental

The samples investigated were identified by X-ray powder diffraction. X-ray data show that the aeschynite-(Y) is completely metamict. A few weak diffraction lines in the unheated polycrase-(Y) indicate that it is almost completely metamict. Both minerals were heated to regain their crystal structure, and to obtain X-ray-diffraction patterns suitable for phase identification and unit-cell measurements. The potentially crucial temperatures for structural restoration were determined from previous investigations (Arnott 1950, Berman 1955, Ewing & Ehlmann 1975) and from the data of thermogravimetric (TGA) and differential thermal analyses (DTA).

Both samples were heated in a muffle furnace in air for 24 hours at 400, 500, 650, 800 and 1000°C. The X-ray powder-diffraction data were collected on Philips PW 3040/60 X'Pert PRO powder diffractometer. The experiments employed Cu$K\alpha$ radiation (λ = 1.54055 Å) at 40 kV and 40 mA. On the incident beam optics, we used divergence slit of ½°. The samples were placed on a disk made of a single crystal of silicon cut in a way to avoid lattice planes and thus providing no diffraction by the silicon and thus a low background. The disk with a sample was inserted into the sample spinner programmed for one revolution per second. Step size was set to 0.02°, with measurement time set at two seconds per step. X-ray-diffraction patterns in the range 31.75–32.75° 2θ were fitted by a pseudo-Voigt function, in order to measure full width at half maximum (FWHM) and intensity. The fitted range corresponds to the position of the 131 reflection of aeschynite, *i.e.*, the 020 reflection of euxenite.

Owing to the great similarity in the diffraction patterns, the chemical composition is crucial for the accurate determination of aeschynite-(Y) and to distinguish polycrase-(Y) from euxenite-(Y). The chemical composition of the samples was obtained by ARL ICP–AES 3520 spectrometer in sequential mode using a specially constructed nebulizer for solutions of high salt content. The emission lines were selected following the criteria of minimal interference and maximal sensitivity. All the lines were checked for interferences of REE with matrix elements; thus the final selection of lines was highly adapted to the composition of the minerals investigated. The samples were not analyzed for La and Pr because of serious interferences with Th and Nb, respectively, and unfavorable signal-to-background ratio. Terbium and Tm were below the detection limit. The instrument was calibrated with a set of REE single-element standard solutions prepared from high-purity REE oxides. For matrix elements, a set of multielement (Ca, Nb, Ti) and single-element (U, Th, Ta) standard solutions was prepared from stock solutions. Since both aeschynite-(Y) and polycrase-(Y) are not easily dissolved in mineral acids, they were fused with high-purity lithium metaborate at 950°C with a sample-to-flux ratio of 1:4. The melted mixture was dissolved in 1.4 mol/dm^3 nitric acid.

Raman spectra were recorded using a computerized DILOR Z24 triple monochromator with Coherent INNOVA 100 argon-ion laser, operating at the 514.5 nm line for excitation. The application of other lines was not considered to be crucial in this study, as Pascoal *et al.* (2003) showed that by using the 514.5 nm laser line, Raman bands are separated from the bands with an electronic origin in spectra of synthetic $REETiTaO_6$ ceramics similar in composition to the minerals investigated. An Anaspec double-pass prism premonochromator was used to reduce parasite laser-plasma lines. A laser power of 100 mW was applied. To reduce the heating of the sample while recording the Raman spectra, the shape of the incident laser beam was altered in line focus. Raman spectra were recorded from 70 to 1600 cm^{-1}. Raman spectra in the range 340–490 cm^{-1} were fitted with a

pseudo-Voigt function in order to measure FWHM and the intensity of the Raman band near 400 cm^{-1} that is related to the Y–O stretching mode.

Thermal analyses were performed for comparison purposes in nitrogen and oxygen atmospheres. The data obtained were used for the determination of heating temperature and H_2O content, but also to characterize possible chemical and physical processes occurring during heating. TGA and DTA curves were recorded in the range from the room temperature up to 1000°C at a heating rate of 5°C/min on a TA Instruments SDT Model 2960.

X-Ray Powder-Diffraction And Thermal Analysis Data

Aeschynite-(Y)

The applied stepwise heating causes the gradual recrystallization of aeschynite-(Y) starting at 400°C, as indicated by the respective powder-diffraction patterns (Fig. 1a). As the temperature rises, the diffraction maxima become sharper and more intense, indicative of the reconstruction of the crystal structure. The FWHM and intensity values (Table 1) generally indicate a trend of FWHM decrease and intensity increase as temperature rises, with a discontinuity in the temperature range from 500 to 650°C. The initial patterns indicate that the mineral starts to recrystallize with the aeschynite structure, which is dominant continuously up to 1000°C. However, the sharp peak at approximately 29.9° 2θ (d = 2.99 Å) becomes more intense at 800°C and finally, at 1000°C, it is dominant over the strongest line for aeschynite at 30.7° 2θ (d = 2.91 Å), suggesting the initiation of a transformation to the euxenite structure. The changes in crystal structure were monitored by calculation of the unit-cell parameters (Table 1). For the aeschynite structure, the a and b parameters increase and the c parameter decreases as temperature rises. Consequently, the unit-cell volume increases, but only up to 800°C, and then it decreases, probably indicating the initiation of a transition to the euxenite structure, which has a smaller unit-cell.

The TGA curve for aeschynite-(Y) (Fig. 2a) clearly indicates dehydration, which is completed around 800°C. The DTA curve (Fig. 2a) shows that recrystallization occurs simultaneously with dehydration. Two exothermic peaks around 400° and 800°C are related to the recrystallization of aeschynite and the beginning of the phase transition to euxenite, respectively. The processes revealed by the TGA–DTA curves influence the

TABLE 1. UNIT-CELL PARAMETERS OF AESCHYNITE-(Y) AND POLYCRASE-(Y) AT DIFFERENT TEMPERATURES, CALCULATED FOR THE DOMINANT STRUCTURE, INDICATED BY THE SPACE-GROUP SYMBOL (*Pbnm*: AESCHYNITE STRUCTURE, *Pbcn*: EUXENITE STRUCTURE)

T°C	space group	*a*	*b*	*c*	*V*	FWHM	Int.
			Aeschynite-(Y)				
400	*Pbnm*	5.180(1)	10.864(3)	7.428(2)	417.9(1)	0.3289	131
500	*Pbnm*	5.182(2)	10.873(3)	7.418(2)	418.0(2)	0.2918	103
650	*Pbnm*	5.181(2)	10.903(5)	7.399(3)	418.0(2)	0.5485	112
800	*Pbnm*	5.190(2)	10.956(3)	7.396(3)	420.6(2)	0.3819	238
1000	*Pbnm*	5.194(2)	10.930(3)	7.386(2)	419.3(2)	0.3269	276
			Polycrase-(Y)				
400	*Pbnm*	5.169(2)	10.902(5)	7.417(2)	418.0(2)	0.6735	92
500	*Pbnm*	5.170(2)	10.917(5)	7.416(3)	418.5(2)	1.1464	84
650	*Pbnm*	5.170(4)	10.941(9)	7.393(6)	418.2(2)	0.4717	109
800	*Pbnm*	5.174(2)	10.957(4)	7.394(4)	419.2(3)	0.3855	330
1000	*Pbcn*	14.517(4)	5.546(2)	5.181(1)	417.2(1)	0.2332	644

The FWHM values, given in %2_, and the intensity (int.), in counts, are for the 131 (aeschynite structure) and 020 (euxenite structure) reflections.

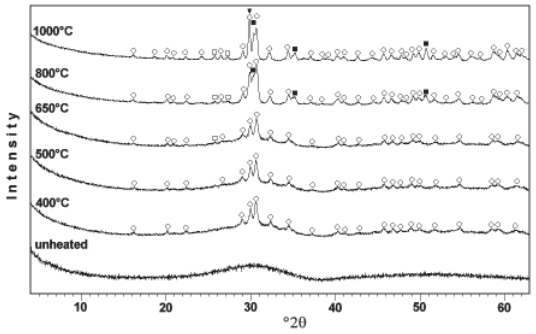

FIG. 1a. Diffraction patterns for unheated and heated aeschynite-(Y), with the following assignments of structure and phases: ○ aeschynite structure, ▼ euxenite structure, ■ pyrochlore, □ brannerite.

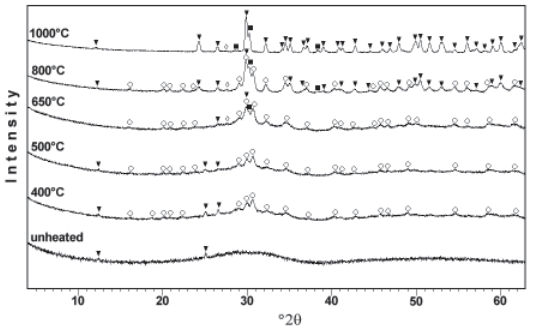

FIG. 1b. Diffraction patterns for unheated and heated polycrase-(Y), with the following assignments of structure and phases: ○ aeschynite structure, ▼ euxenite structure, ■ pyrochlore, □ rutile.

changes in unit-cell parameters. During dehydration, H_2O is expelled from the mineral over an extensive range of temperature, thus most likely imposing a slower recrystallization regime and minor structural readjustments due to the random paths of its escape. In addition, the aeschynite–euxenite phase transition causes changes in unit-cell dimensions.

Aeschynite-(Y) heated at temperatures higher than 650°C also yields some additional diffraction lines, which are not in agreement with the set of diffraction lines possible either for space group *Pbnm* (aeschynite) or for space group *Pbcn* (euxenite). Some of them indicate the presence of a cubic pyrochlore-group phase. The unit-cell dimension of this pyrochlore phase can be estimated on the basis of the few lines observed. In this case, it is approximately a = 10.18 Å. Also, the two strongest reflections of brannerite were observed. The appearance of additional phases upon heating metamict minerals is common (Cesbron 1989), especially in the case of aeschynite- and euxenite-group minerals (Ewing & Ehlmann 1975, Bonazzi *et al.* 2002), such that their primary or secondary origin could be questioned. However, in this case, these other phases were not observed in the original mineral.

The transformation from the aeschynite to the euxenite structure discussed here was observed in previous investigations (Komkov 1972, Ewing & Ehlmann 1975, Bonazzi *et al.* 2002). The aeschynite structure is stable for the whole REE group in compounds of the type AB_2O_6, whereas the euxenite structure is stable only for the heavy rare-earth elements (HREE), and it is a high-temperature phase (Komkov 1972). However, the aeschynite–euxenite transition seems to be incomplete in this case, since aeschynite is still the dominant phase at 1000°C, as indicated by the X-ray-diffraction pattern.

Polycrase-(Y)

The unheated polycrase-(Y) is largely metamict, although two weak diffraction lines at 12.4° 2θ (d = 7.12 Å) and 25.1° 2θ (d = 3.54 Å) can be seen (Fig. 1b). Impurities were not observed in the mineral. These two peaks are very likely a remnant of the original pre-metamict structure, as indicated by the line at 12.4° 2θ (d = 7.12 Å) characteristic of the 200 plane of the euxenite structure. Also, the 25.1° 2θ line (d = 3.54 Å) could be caused by the highly disturbed but partially preserved 400 plane of the same structure. The gradual

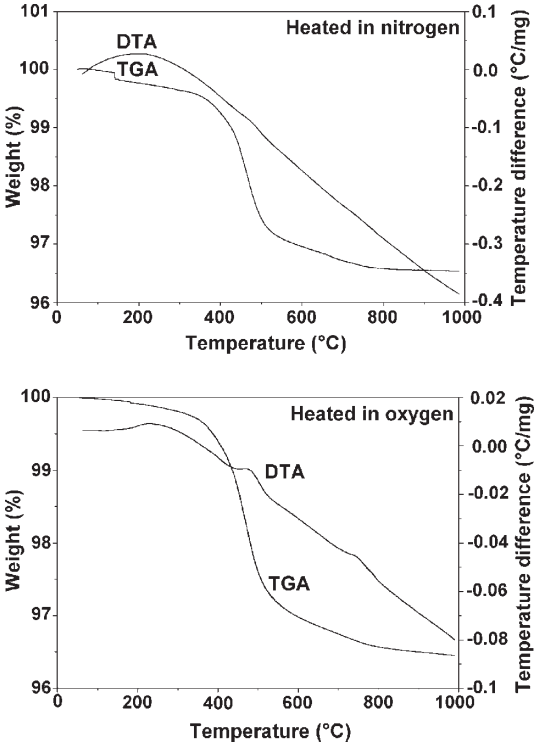

FIG. 2a. TGA–DTA diagrams for aeschynite-(Y).

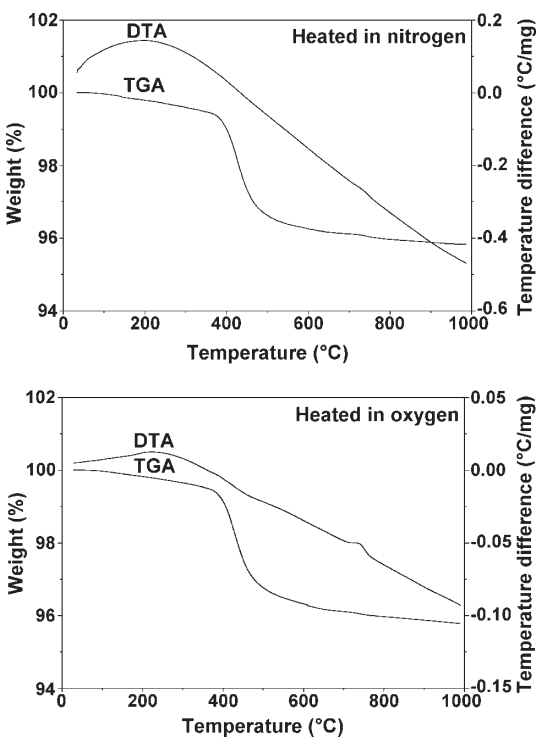

FIG. 2b. TGA–DTA diagrams for polycrase-(Y).

recrystallization starts at 400°C and could be continuously monitored up to 1000°C (Fig. 1b). With the increase of temperature, the intensities increase and the diffraction lines narrow, which can be also inferred from the FWHM and intensity values (Table 1). As observed in the case of aeschynite-(Y), there is a discontinuity in this trend also, here at 500°C. In both cases, this discontinuity occurs in the step preceding the euxenite–aeschynite transformation. This observation could be related to the beginning of the structural re-arrangement in the incompletely recrystallized mineral. The mineral firstly recrystallizes dominantly with the aeschynite structure, which is stable up to 800°C. At 650°C, the first indications of a transition to the euxenite structure appear, as the strongest of the diffraction lines of euxenite at 29.9° 2θ (d = 2.99 Å) becomes dominant, and the aeschynite peaks start to decrease in intensity. This trend becomes more pronounced at 800°C, as other diffraction lines of euxenite start to appear. At 1000°C, the aeschynite structure completely disappears, and polycrase with the euxenite structure is the stable phase.

TGA–DTA diagrams confirm the processes observed by X-ray diffraction. Dehydration is completed at around 600°C (Fig. 2b), which is a lower temperature than the one observed for aeschynite-(Y). The indications of the structural transformation could be observed in DTA curves, which are significantly more pronounced when the sample is heated in an oxygen atmosphere (Fig. 2b). The exothermic peak around 400°C, which is related to the beginning of recrystallization of the aeschynite structure, is less pronounced than the one around 800°C corresponding to the aeschynite–euxenite phase transition.

The unit-cell parameters show the same trend of changes with temperature increase as observed in the case of aeschynite-(Y) (Table 1). These changes are presumably associated with the same processes induced by heating. The final unit-cell volume of polycrase-(Y) with the euxenite structure calculated for the mineral heated at 1000°C confirms the assumption about the initial stage of aeschynite–euxenite transition for aeschynite-(Y) in the temperature range 800–1000°C, where the unit-cell volume starts to decrease. However, the overlap of the diffraction lines related both to the aeschynite and euxenite structure, such as the strong line approximately at 29.9° 2θ (d = 2.99 Å), makes the phase recognition and thus the calculation of the unit-cell parameters difficult, especially at the temperatures at which the transition is not completed. In addition, a pyrochlore phase becomes observable at 650°C, *i.e.*, at a lower temperature than in the case of aeschynite-(Y). It is represented by an estimated unit-cell with $a \approx 10.24$ Å. The weak peak around 27.5° 2θ (d = 3.24 Å) probably indicates the presence of a rutile phase above 650°C.

TABLE 2. CHEMICAL COMPOSITION OF AESCHYNITE-(Y) AND POLYCRASE-(Y)

	Aeschynite-(Y)		Polycrase-(Y)			Aes	Plc
CaO wt%	1.10	(1.82)	2.75	(2.21)	Ca *apfu*	0.075	0.188
ThO_2	8.61	(1.57)	3.87	(1.99)	Th	0.125	0.056
UO_2 *	4.78	(2.38)	12.87	(1.87)	U	0.068	0.183
Ce_2O_3	0.94	(3.38)	0.33	(4.01)	Ce	0.022	0.008
Nd_2O_3	2.10	(1.88)	0.55	(2.50)	Nd	0.048	0.012
Sm_2O_3	1.56	(0.31)	0.61	(2.28)	Sm	0.034	0.013
Gd_2O_3	1.72	(3.11)	1.16	(3.32)	Gd	0.036	0.025
Dy_2O_3	2.00	(3.07)	2.15	(5.43)	Dy	0.041	0.044
Ho_2O_3	0.45	(2.58)	0.56	(2.22)	Ho	0.009	0.011
Er_2O_3	1.38	(2.95)	1.71	(4.51)	Er	0.028	0.034
Yb_2O_3	1.89	(1.70)	2.26	(1.64)	Yb	0.037	0.044
Lu_2O_3	0.34	(4.21)	0.46	(1.70)	Lu	0.006	0.009
Y_2O_3	14.15	(0.40)	13.77	(2.72)	Y	0.480	0.468
					A cations	1.009	1.095
TiO_2	29.34	(1.81)	24.78	(2.25)	Ti	1.405	1.190
Nb_2O_5	16.75	(0.90)	24.47	(1.91)	Nb	0.482	0.706
Ta_2O_5	9.53	(1.67)	4.27	(0.44)	Ta	0.165	0.074
					B cations	2.052	1.970
H_2O **	3.50		4.10				
Total	100.14		100.67				

The number of cations, given in atoms per formula unit (*apfu*), is calculated on the basis of six atoms of oxygen. The analytical errors are given as a relative standard deviation in %, and shown in parentheses. * The oxidation state of uranium was not determined. ** Excluded from cation-assignment calculation.

Chemical Composition

The results of the chemical analyses of aeschynite-(Y) and polycrase-(Y) are given in Table 2, together with cation assignments. The analytical errors are expressed as relative standard deviations of three measurements performed for each sample [RSD = 100 (σ / $\bar{x}$)], where σ is standard deviation, and $\bar{x}$, the arithmetic mean of the multiple measurements). The simplified structural formula of aeschynite-(Y) can be written as $(Y_{0.48}Ln_{0.26}Th_{0.12}U_{0.07}Ca_{0.08})_{\Sigma 1.01}(Ti_{1.40}Nb_{0.48}Ta_{0.16})_{\Sigma 2.04}O_6$, and that of polycrase-(Y), as $(Y_{0.47}Ln_{0.20}Ca_{0.19}U_{0.18}Th_{0.06})_{\Sigma 1.10}(Ti_{1.19}Nb_{0.71}Ta_{0.07})_{\Sigma 1.97}O_6$ (Ln: lanthanides). The formulae show both minerals to have Y and Ti as dominant *A*- and *B*-site cations, respectively. The predominance of Ti at the *B* site distinguishes polycrase-(Y) from euxenite-(Y), which has Nb as the dominant *B*-site cation. Obviously, the dominant cations do not differ between aeschynite-(Y) and polycrase-(Y). Ewing (1976) used a canonical discriminant analysis to distinguish between euxenite- and aeschynite-group minerals. He proposed that the total of uranium oxides and ThO_2 could be used as a criterion to distinguish between aeschynite-(Y) and euxenite-(Y). If the sum of uranium oxides is greater than ThO_2, the mineral should be classified as euxenite-(Y). Since polycrase-(Y) belongs to the euxenite group, Hanson *et al.* (1992, 1998) by analogy proposed the same criterion to distinguish between aeschynite-(Y) and polycrase-(Y). Thus, the content of UO_2 and ThO_2 for the investigated minerals (Table 2) distinguishes polycrase-(Y) from aeschynite-(Y). However, if ThO_2 dominates over the sum of ura-

nium oxides, the nomenclature is ambiguous (Ewing 1976).

Raman Spectra

The Raman spectrum for aeschynite-(Y) at room temperature gives evidence of the lack of crystallinity, with only few broad vibration bands present. The gradual increase of crystallinity following the temperature increase observed in diffraction patterns was also observed with Raman spectroscopy (Fig. 3a). The bands become better resolved and less broad after heating the mineral to higher temperatures, as seen from the FWHM and intensity values (Table 3). Raman bands appeared in the region from 70 to 900 cm^{-1}, whereas all higher-frequency bands have an electronic origin (Paschoal *et al.* 2003).

The recrystallization of polycrase-(Y) with an increase in temperature was also indicated by Raman spectroscopy (Fig. 3b, Table 3). Moreover, the phase transition revealed by XRD in the temperature range from 650° to 800°C was confirmed. The position and relative intensity of the broad bands recorded in the region 200–550 cm^{-1} after heating at 650°C can be explained in terms of the coexistence of euxenite and aeschynite structure-types. In the spectrum recorded for the mineral heated at 800°C, the bands associated with the euxenite structure become more intense. In the mineral heated at 1000°C, bands at 255, 305 and 360 cm^{-1} related to aeschynite were not observed in the Raman spectrum. However, the broad bands with a maximum intensity at 224 and 404 cm^{-1} might be explained as the superposition of euxenite and aeschynite bands in light of the Raman results of Paschoal *et al.* (2003).

Assignment of Raman bands

The factor-group analysis predicts 54 Raman-active modes in the aeschynite and also in the euxenite structure (Paschoal *et al.* 2003). We observed a smaller number of modes, probably due to broadening of the bands, which masked weaker bands (Figs. 3a, b). The band assignment is not easy in complex oxides, and a different approach was used to assign Raman modes. Generally, it was found that the polymorphs of Nb_2O_5 consist of "different types of niobium–oxygen polyhedra, predominantly corner-shared and edge-shared NbO_6 octahedra" (McConnell *et al.* 1976). In our interpretation of the Raman bands, the internal mode approach was found here to be convenient, *i.e.*, that taking mostly into consideration the internal vibrations in metal–oxygen polyhedra. Following the assignment of bands in niobium oxides (McConnell *et al.* 1976), it was possible to identify some bands (Table 4). The two bands in the region 650–900 cm^{-1}, characteristic of both samples investigated, may be assigned to *B*–O stretching in BO_6 octahedra. The bands are broad and asymmetric, indicating distortion along the stacking of the BO_6 (*B* = Nb, Ti, Ta) polyhedra. This distortion is expected owing to the incorporation of different cations at the *B* site. Moreover, it could also indicate random distribution of cat-

TABLE 3. FWHM AND INTENSITY OF THE RAMAN BAND AT AROUND 400 cm^{-1} (Y–O STRETCHING MODE) IN AESCHYNITE-(Y) AND POLYCRASE-(Y)

T°C	Aeschynite-(Y)		Polycrase-(Y)	
	FWHM	Int.	FWHM	Int.
400	45.1	152	44.3	146
500	43.5	250	43.7	156
650	41.9	693	40.2	175
800	32.3	1986	31.8	444
1000	31.8	2013	27.5	1042

FWHM is expressed in cm^{-1}, and the intensity (Int.), in counts.

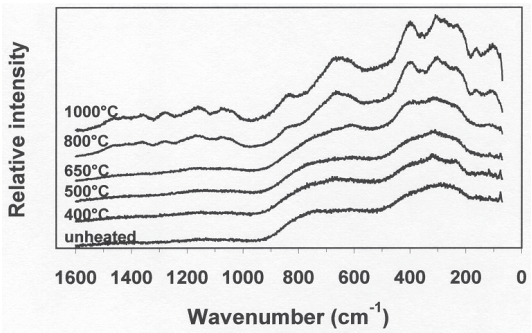

FIG. 3a. Raman spectra for unheated and heated aeschynite-(Y).

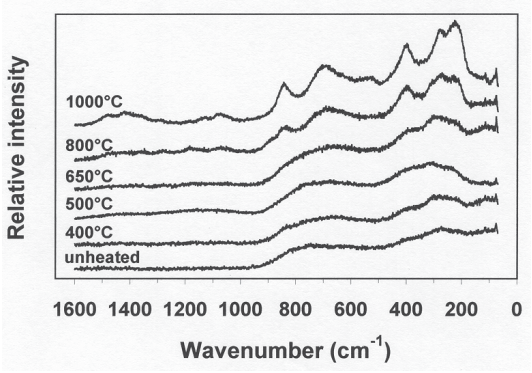

FIG. 3b. Raman spectra for unheated and heated polycrase-(Y).

ions at the *B* site. Concerning the investigation of Dobal *et al.* (2001), the frequency bands with wavenumber greater than 450 cm^{-1} could be associated with the modes involving mainly the stretching of the various Ta–O or Ti–O bonds present in the structure, with different magnitude of bond order. Raman bands between 200 and 450 cm^{-1} generally correspond to the O–Ta–O and O–Ti–O bending and Ti–O stretching. The positions of bands in the region from 200 to 550 cm^{-1} in aeschynite-(Y) suggest that the material crystallized as a mixture of aeschynite and euxenite (Fig. 3a, Table 4), in view of the results of Paschoal *et al.* (2003). They investigated synthetically prepared $REETiTaO_6$ ceramics using Raman spectroscopy and found that the structure is dependent on the REE component. The ceramics with REE = Ce, Pr, Nd, Sm, Eu, Gd and Dy have the aeschynite structure, and the ceramics with REE = Y, Ho, Er and Yb have the euxenite structure. In our work, the natural minerals had various REE present at site *A*, along with dominant Y (Table 2), so presumably both structures were possible, which is in agreement with the findings of Komkov (1972). A comparison of the investigated Raman spectra could also be made with those of simple synthetic rare-earth oxides with the C-type structure [α-Mn_2O_3 structure (bixbyite), space group *Ia*3] (White & Keramidas 1972, Tucker *et al.* 1984). In that respect, the strong band appearing in the range 380–400 cm^{-1} may be related to Y–O vibration. Also, Raman bands below 200 cm^{-1} are probable lattice vibrations related to REE ions (Paschoal *et al.* 2003).

TABLE 4. RAMAN BANDS FOR AESCHYNITE-(Y) AND POLYCRASE-(Y) HEATED AT 1000%C

Aeschynite-(Y)			Polycrase-(Y)		
Wave-number	Phase[1]	Band assignment	Wave-number	Phase[1]	Band assignment
99					
			117		
159					
212	Eux		224	Eux	
232	Aes			& Aes	
256	Aes				
277	Eux	Ta–O	272	Eux	Ta–O
302	Eux				
	& Aes				
355	Aes				
396	Aes	Y–O stretching	404	Aes	Y–O stretching
	& Eux			& Eux	
			522		Ta–O stretching
			542	Eux	Ta–O stretching
609		Ta–O stretching			
665		TO* Nb–O stretching	685		TO* Nb–O stretching
830		LO** Nb–O stretching	840		LO** Nb–O stretching
1058		luminescence	1068		luminescence
			1122		
1145			1176		
1265			1282		
1347			1351		
1409			1414		
1451			1465		

[1] By comparison with work of Paschoal *et al.* (2003).
* transversal optical mode; ** longitudal optical mode.
Symbols: Aes: aeschynite, Eux: euxenite. Wavenumbers expressed in (cm^{-1}).

Discussion

Owing to their complicated paths of recrystallization induced by heating and their mutual similarities, it is very difficult to correctly identify the metamict complex oxides of Nb, Ta, Ti and REE. These problems are especially troublesome in the description of aeschynite- and euxenite-group minerals owing to their close chemical and structural features. Although these minerals have the same stoichiometry, they are not usually considered as polymorphs, because of wide and complex substitutions. Therefore, naturally occurring samples do not commonly have a close chemical content.

X-ray-diffraction experiments of metamict Nb–Ta–Ti–REE oxide minerals without systematic heating procedures could in some cases be misleading. However, by obtaining diffraction data over an extensive range in temperature, it is possible to get valuable information on recrystallization sequences and accompanying transformations of crystal structure.

Sensitivity of X-ray-diffraction and Raman spectroscopy to the changes of crystal structure during recrystallization of metamict Nb–Ta–Ti–REE oxide minerals

Raman spectra obtained here for aeschynite-(Y) and polycrase-(Y) generally confirm the great similarities between these two minerals. As seen through X-ray-diffraction experiments, this spectral similarity is largely due to the transformation during heating experiments from the aeschynite to the euxenite structure in both minerals. Some vibration frequencies of the investigated minerals are found to be common to both of them (Table 4). This similarity could reflect similar atom positions and cation coordination in the crystal structure. Indeed, Nb, Ta and Ti in the minerals here concerned are typically coordinated with six atoms of oxygen, *i.e.*, they form NbO_6, TaO_6 and TiO_6 octahedral groups. On the other hand, the REE, as larger cations, are coordinated by eight oxygen atoms, usually forming square antiprism (Aleksandrov 1962, Černý & Ercit 1989, Miyawaki & Nakai 1996).

However, the possible distortion and stacking of polyhedra are not necessarily the same (Figs. 4a, b), and this can produce differences in vibration spectra. These differences are characteristic for the wavenumber region 200–550 cm^{-1} of the Raman spectra of the two samples investigated here, and that is also the case with the corresponding synthetic compounds (Paschoal *et al.* 2003). In the aeschynite structure, the BO_6 octahedra are joined at an edge in pairs, which are then mutually connected

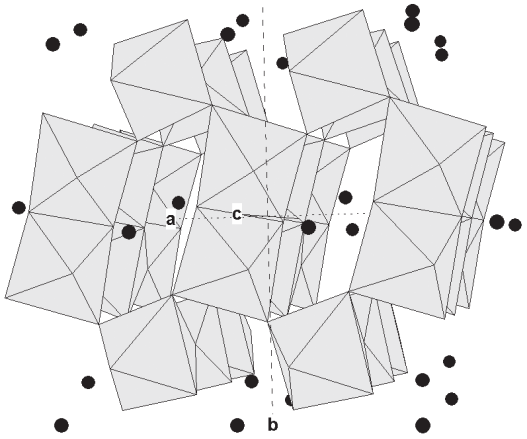

FIG. 4a. Crystal structure of aeschynite-(Y) (after Aleksandrov 1962). Black circles represent *A*-site cations, and the *B*-site cations are octahedrally coordinated.

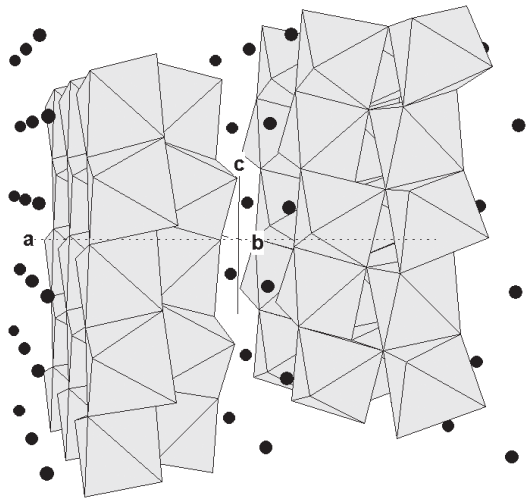

FIG. 4b. Crystal structure of polycrase-(Y) (after Aurisicchio *et al.* 1993). Black circles represent *A*-site cations, and the *B*-site cations are octahedrally coordinated.

at corners in a zigzag pattern to form double chains along the *c* axis (Fig. 4a, after Aleksandrov 1962). During the transformation to the euxenite structure, the BO_6 octahedra re-arrange themselves into double layers stacked parallel to *c* axis, being joined both by edge- and corner-sharing (Fig. 4b, after Aurisicchio *et al.* 1993). These changes generally influence bond lengths and distortions for both BO_6 and AO_8 coordination polyhedra.

The structure transformation is also responsible for the shift of TO and LO modes (Table 4). The features of the region 200–550 cm^{-1} are possibly a powerful tool in mutually distinguishing the phases with the aeschynite and the euxenite structure, being a fingerprint of sorts. Morever, the Raman data collected in the wavenumber region 70–200 cm^{-1} indicate that it might be possible to trace the remnants of the pre-existing structure when it is not visible to X-rays any longer, as was the case with final transformation of the polycrase-(Y) to the euxenite structure at 1000°C. However, it remains unclear how additional phases like pyrochlore, brannerite or rutile, appearing during heating, influence these Raman spectra in general. In addition, comparison with corresponding synthetic end-members, due to their chemically restricted selection of cations, could be in some instances of limited relevance.

Structural transformations observed for both minerals in their XRD patterns and Raman spectra, are also supported by DTA. The exothermic peaks occurring at temperatures corresponding to the transition of the metamict state to the aeschynite structure (around 400°C) and to the aeschynite–euxenite transformation (around 800°C) are present on DTA curves recorded both in oxygen and nitrogen atmosphere. However, the effects of these processes are less prominent in a nitrogen atmosphere. So, for the samples heated in air prior to XRD and Raman analysis, the magnitude of these effects should be somewhat intermediate. These DTA data are very interesting in evaluating the influence of the atmosphere on the heated minerals. In general, heating procedures in this work followed the previous work of Ewing & Ehlman (1975), who had heated euxenite samples in air in accordance with the findings of Hutton (1961), who had observed no differences in the X-ray patterns of the euxenite samples heated in air and in vacuum.

Finally, for the samples of aeschynite-(Y) and polycrase-(Y), Raman spectra do not show the presence of structural fragments possibly preserved in the metamict state. X-ray-diffraction experiments support the Raman data indicating that the unheated minerals are metamict. Only in the case of polycrase-(Y) do two weak diffraction lines indicate a pre-metamict crystal structure. Especially interesting is the weak line at approximately 12.4° 2θ (d = 7.12 Å), which disappears during heating and then re-appears as the transformation to the euxenite structure takes place. This reflection is a relic of incompletely metamict euxenite-type structure and a good criterion with which to recognize a metamict mineral with an originally euxenite-type structure.

ACKNOWLEDGEMENTS

Sincere thanks go to Dr. Gunnar Raade from Geological Museum of the University of Oslo for providing

us with the mineral samples. The authors are especially thankful to Prof. Dr. Ilse Steffan from the Institute of Analytical Chemistry of the University of Vienna for her help and support in the mineral chemical analysis. We thank A.M. Seydoux-Guillaume and R.F. Martin for their reviews and suggestions, which significantly improved the manuscript. A part of this work was supported by the Ministry of Science and Technology of the Republic of Croatia through the Grant 0119420 and 0098022.

References

ALEKSANDOV, V.B. (1962): The crystal structure of aeschynite. *Dokl. Akad. Nauk SSSR* **142**, 181-184 (in Russ.).

ARNOTT, R.J. (1950): X-ray diffraction data on some radioactive oxide minerals. *Am. Mineral.* **35**, 386-400.

AURISICCHIO, C., ORLANDI, P., PASERO, M. & PERCHIAZZI, N. (1993): Uranopolycrase, the uranium-dominant analogue of polycrase-(Y), a new mineral from Elba Island, Italy, and its crystal structure. *Eur. J. Mineral.* **5**, 1161-1165.

BERMAN, J. (1955): Identification of metamict minerals by X-ray diffraction. *Am. Mineral.* **40**, 805-827.

BOLDISH, S.I. & WHITE, W.B. (1979): Vibrational spectra of crystals with the A-type rare earth oxide structure. I. La_2O_3 and Nd_2O_3. *Spectrochim. Acta* **A35**, 1235-1242.

BONAZZI, P., ZOPPI, M. & DEI, L. (2002): Metamict aeschynite-(Y) from the Evje–Iveland district (Norway): heat-induced recrystallization and dehydrogenation. *Eur. J. Mineral.* **14**, 141-150.

BUGGE, J.A.W. (1978): Norway. *In* Mineral Deposits of Europe **1**: Northwest Europe (S.H.U. Bowie, A. Kvalheim & H.W. Haslam, eds.). The Institution of Mining and Metallurgy & The Mineralogical Society, London, UK (199-249).

BYEON, SONG-HO, LEE, SUNG-OKH & KIM, HONGDOO (1997): Structure and Raman spectra of layered titanium oxides. *J. Solid State Chem.* **130**, 110-116.

ČERNÝ, P. & ERCIT, T.S. (1989): Mineralogy of niobium and tantalum: crystal chemical relationships, paragenetic aspects and their economic implications. *In* Lanthanides, Tantalum and Niobium: Mineralogy, Geochemistry, Characteristics of Primary Ore Deposits, Prospecting, Prodessing and Applications (P. Möller, P. Černý & F. Saupé, eds.). Springer-Verlag, Berlin, Germany (27-79).

CESBRON, F.P. (1989): Mineralogy of the rare-earth elements. *In* Lanthanides, Tantalum and Niobium: Mineralogy, Geochemistry, Characteristics of Primary Ore Deposits, Prospecting, Processing and Applications (P. Möller, P. Černý & F. Saupé, eds.). Springer-Verlag, Berlin, Germany (3-26).

DOBAL, P.S., KATIYAR, R.S., JIANG, Y., GUO, R. & BHALLA, A.S. (2001): Structural modifications in titania-doped tantalum pentoxide crystals: a Raman scattering study. *Int. J. Inorg. Mater.* **3**, 135-142.

EWING, R.C. (1975): The crystal chemistry of complex niobium and tantalum oxides. IV. The metamict state: discussion. *Am. Mineral.* **60**, 728-733.

_____ (1976): A numerical approach toward the classification of complex, orthorhombic, rare-earth, AB_2O_6-type Nb–Ta–Ti oxides. *Can. Mineral.* **14**, 111-119.

_____ (1987): The structure of the metamict state. *In* 2nd Int. Conf. on Natural Glasses (Prague) (J. Konta, ed.). Charles University, Praha, Czech Republic (41-48).

_____ & EHLMANN, A.J. (1975): Annealing study of metamict, orthorhombic rare earth, AB_2O_6- type, Nb–Ta–Ti oxides. *Can. Mineral.* **13**, 1-7.

_____, WEBER, W.J. & CLINARD, F.W., JR. (1995): Radiation effects in nuclear waste forms for high-level radioactive waste. *Progr. Nucl. Energy* **29**, 63-127.

GÖGEN, K. & WAGNER, G.A. (2000): Alpha-recoil track dating of Quaternary volcanics. *Chem. Geol.* **166**, 127-137.

GRAHAM, J. & THORNBER, M.R. (1974): The crystal chemistry of complex niobium and tantalum oxides. IV. The metamict state. *Am. Mineral.* **59**, 1047-1050.

HANSON, S.L., SIMMONS, W.B., JR. & FALSTER, A.U. (1998): Nb–Ta–Ti oxides in granitic pegmatites from the Topsham pegmatite district, southern Maine. *Can. Mineral.* **36**, 601-608.

_____, _____, WEBBER, K.L. & FALSTER, A.U. (1992): Rare-earth-element mineralogy of granitic pegmatites in the Trout Creek Pass pegmatite district, Chaffee County, Colorado. *Can. Mineral.* **30**, 673-686.

HUTTON, C.O. (1961): Contributions to the mineralogy of New Zealand V. *Trans. R.Soc. New Zealand* **88**, 639-653.

KOMKOV, A.I. (1972): Polymorphic relationships in compounds of $TRNbTiO_6$ and $TRTaTiO_6$ types. *Dokl. Akad. Nauk SSSR* **206**(6), 1353-1354 (in Russ.).

LIMA-DE-FARIA, J. (1958): Heat treatment of metamict euxenites, polymignites, yttrotantalites, samarskites, and allanites. *Mineral. Mag.* **31**, 937-942.

_____ (1962): Heat treatment of chevkinite and perrierite. *Mineral. Mag.* **33**, 42-47.

MCCONNELL, A.A., ANDERSON, J.S. & RAO, C.N.R. (1976): Raman spectra of niobium oxides. *Spectrochim. Acta* **A32**, 1067-1076.

MENG, J.F., RAI, B.K., KATIYAR, R.S. & BHALLA, A.S. (1997): Raman investigation on $(Ta_2O_5)_{1-x}(TiO_2)_x$ system at different temperatures and pressures. *J. Phys. Chem. Solids.* **58**, 1503-1506.

MIYAWAKI, R. & NAKAI, I. (1996): Crystal chemical aspects of rare earth minerals. *In* Rare Earth Minerals (A.P. Jones, F. Wall & C.T. Williams, eds). Chapman & Hall, London, U.K. (21-40).

NASDALA, L., IRMER, G. & WOLF, D. (1995): The degree of metamictization in zircon: a Raman spectroscopic study. *Eur. J. Mineral.* **7**, 471-478

_____, LENGAUER, C.L., HANCHAR, J.M., KRONZ, A., WIRTH, R., BLANC, P., KENNEDY, A.K. & SEYDOUX-GUILLAUME, A.-M. (2002): Annealing radiation damage and the recovery of cathodoluminescence. *Chem. Geol.* **191**, 121-140.

NEUMANN, H. & SVERDRUP, T.L. (1960): Contribution to the mineralogy of Norway. 8. Davidite from Tuftan, Iveland. *Norsk Geol. Tidsskr.* **40**, 277-288.

PASCHOAL, C.W.A., MOREIRA, R.L., FANTINI, C., PIMENTA, M.A., SURENDRAN, K.P. & SEBASTIAN, M.T. (2003): Raman scattering study of $RETiTaO_6$ dielectric ceramics. *J. Eur. Ceram. Soc.* **23**, 2661-2666.

PODOR, R. (1995): Raman spectra of the actinide-bearing monazites. *Eur. J. Mineral.* **7**, 1353-1360.

SEYDOUX-GUILLAUME, A.M. (2001): *Experimental Determination of the Incorporation of Th into Orthophosphate and the Resetting of Geochronological Systems of Monazite.* Ph.D. thesis, Technische Universität Berlin, Berlin, Germany.

_____, WIRTH, R., NASDALA L., GOTTSCHALK, M., MONTEL, J.M. & HEINRICH, W. (2002): An XRD, TEM and Raman study of experimentally annealed natural monazite. *Phys. Chem. Minerals* **29**, 240-253.

TUCKER, L.A., CARNEY, F.J., JR., MCMILLAN, J.R.P., LIN, S.H. & EYRING, L. (1984): Raman and resonance Raman spectroscopy of selected rare-earth sesquioxides. *Appl. Spectros.* **38**, 857-860.

WHITE, W.B. & KERAMIDAS, V.G. (1972): Vibrational spectra of oxides with the C-type rare earth oxide structure. *Spectrochim. Acta* **A28**, 501-509.

YASHIMA, M., LEE, JIN-HO, KAKIHANA, M. & YOSHIMURA, M. (1997): Raman spectral characterization of existing phases in the Y_2O_3–Nb_2O_5 system. *J. Phys. Chem. Solids* **58**, 1593-1597.

Received December 21, 2003, revised manuscript accepted September 8, 2004.